RESULT IN NEUTRINO OSCILLATIONS FROM 400-DAYS DATA OF SUPER-KAMIOKANDE

Yoshitaka Itow
Kamioka Observatory
Institute for Cosmic Ray Research, University of Tokyo,Higashi-Mozumi,
Kamioka, Gifu, 506-12, Japan

Representing Super-Kamiokande Collaboration[1]

ABSTRACT

The Super-Kamiokande experiment, using the largest underground water Čerenkov detector, has been running since April 1, 1996. The total live time for the analysis has reached more than 300 days. The newest results in atmospheric neutrino, solar neutrino and related topics are reported.

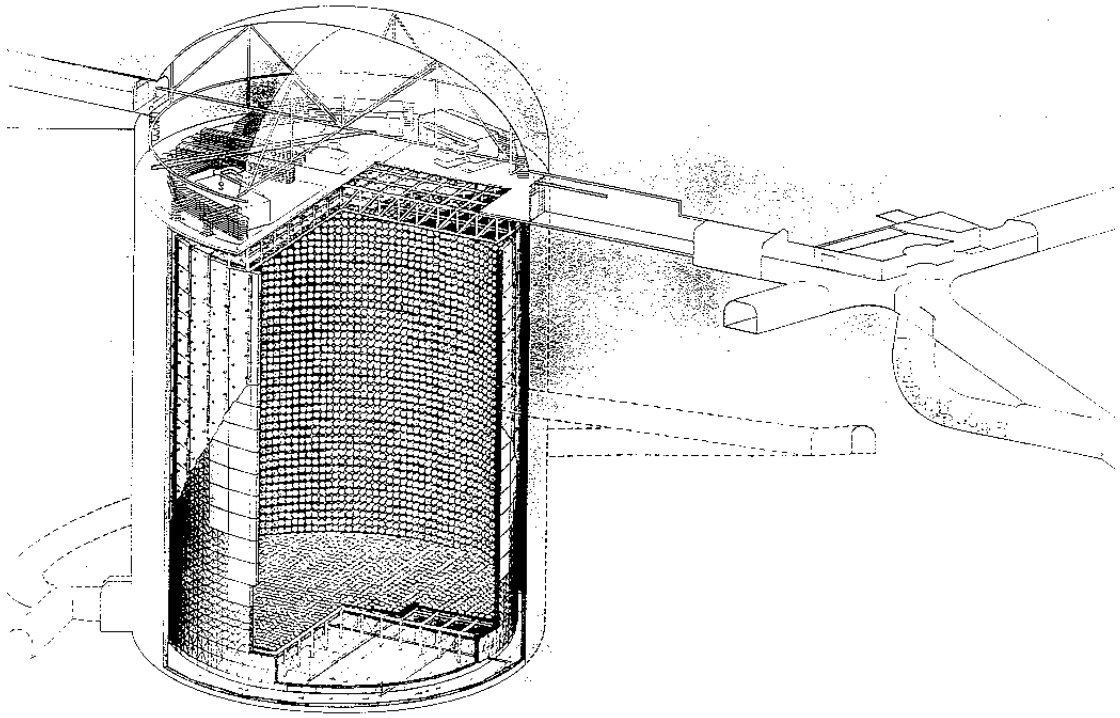

Figure 1: The schematic view of Super-Kamiokande detector.

1 Introduction

The Super-Kamiokande detector is a 50,000 ton water Čerenkov detector located at a depth of 2,700 meters water equivalent in the Kamioka mine in Japan. A schematic view of detector is shown as Fig 1. The detector cavity is 42 m in height and 39 m in diameter, filled with 50,000 tons of pure water. The fiducial mass for the measurement of solar and atmospheric neutrino interactions is 22,000 tons, which is more than 20 times larger than that of Kamiokande. It consists of two layers of detector. The inner tank has 33.8 m diameter and 36.2 m high. 11,146 50 cm ϕ photomultiplier tubes (PMTs), instrumented on all surfaces of the inner detector, detect Čerenkov photons radiated by relativistic charged particles. The outer layer, approximately 2 m thick, is used as an anti-counter where 1,885 20 cm ϕ PMTs is instrumented. The anti-counter is useful for identifying entering cosmic-ray muons and for reducing gamma-rays or neutrons from surrounding rock. Pulse-height and timing information from each PMT are recorded and used in the data analysis.

Super-Kamiokande has been successfully operated without any serious troubles since April 1st, 1996. The detector has been alive in 85 % of the time. Most of the dead time is due to calibrations. The cumulative live-time of operation reached more than 500 days in the fall of 1997. The transparency of water is about 80 m measured by using electrons from μ decay. The trigger threshold had been about 5.6 MeV for electrons at 50% efficiency from the beginning of the experiment. It has been set to about 4.6 MeV since May 1997 to collect a much lower energy data sample. The concentration of Rn in the water is less than 5 m Bq/m^3 which is two order of magnitude lower than that in Kamiokande. The total live-time of data sample for analysis of solar neutrino, up-going μ, atmospheric neutrino and proton decay has reached more than 300 days. Now it is time to obtain the conclusive results in neutrino oscillation studies with large statistics. In the following sections, new results in solar neutrino and in atmospheric neutrino analyses are presented.

2 Solar neutrinos

The Sun maintains its luminosity by the energy of nuclear fusion reactions. Thus the Sun emits low-energy ($E_\nu \leq 15$ MeV) electron neutrinos (ν_e) that are products of the nuclear processes inside the Sun. Our understanding of those processes is reflected in the standard solar model (SSM). The flux and spectrum of neutrinos corresponding to each nuclear process are well predicted by SSM. Figure 2 shows the energy spectra of the solar neutrino flux on the earth calculated by SSM of Bahcall and Pinsonneault in 1995 (BP-95).[2]Also shown are the energy threshold of five current existing solar neutrino experiments, the Homestake experiment,[3] Kamiokande,[4] SAGE,[5] GALLEX[6] and the presented experiment, Super-Kamiokande,[7] in the same figure.

The first observation of the solar neutrino was achieved in the early 1970's by Davis et al. by using of following reactions; $^{37}\mathrm{Cl} + \nu_e \rightarrow ^{37}\mathrm{Al} + e^-$ ($E_\nu \geq$ 0.814 MeV). Their obtained result have shown a significant deficit of the yield compared to predictions based on various versions of the SSM. The SAGE and GALLEX experiments used following reactions; $^{71}\mathrm{Ga} + \nu_e \rightarrow ^{71}\mathrm{Ge} + e$ ($E_\nu \geq 0.233$ MeV). Those experiments can detect much lower energy neutrinos produced via "p-p" chain that maintain most of the Sun's luminosity. The obtained results are about half of the expected one. Kamiokande has performed the first real

time measurement of solar neutrinos by using of water Čerenkov technique. Solar neutrinos can be detected through neutrino-electron scattering, $\nu e \rightarrow \nu e$. The electron energy, direction and the time of the reaction are measured. The obtained result was about 40 % of the expectation.

The flux measurements are summarized in the Table 1. All the experiments showed significantly lower flux than that from the SSM prediction, while the detection methods and the energy thresholds of the measurement are different among each other. It is hard to explain all the existing results consistently with SSM. The solar neutrinos which are expected to be detected in the Homestake experiment are about 80 % from ^{8}B-neutrino and about 15 % from ^{7}Be-neutrino, while only ^{8}B-neutrino can be detected by the water Čerenkov detectors. The obtained Data/SSM in the Homestake experiment is about 1/3, while it is about one half in Kamiokande. This difference suggests almost no contribution from ^{7}Be-neutrino in the Homestake data. On the other hand, the contribution of "p-p"-neutrinos, ^{7}Be-neutrino and ^{8}B-neutrino in the data sample of Ga experiments are expected to be about 50 %, 30 % and 10 %, respectively. The flux of "p-p"-neutrino is constrained by total luminosity of the Sun. It again may suggest strong suppression of ^{7}Be-neutrinos. Those results from the existing experiments hints a possible distortion of energy spectrum of solar neutrinos which can be explained by the hypothesis of $\nu_e \rightarrow \nu_x$ oscillations oscillation. The distance between the earth and the Sun is $\sim 10^{11}$ m and $E_\nu \sim 10$ MeV, so that typical E/L is 10^{-10}. If the Δm^2 is substantially larger than 10^{-10} eV^2, solar neutrinos with any energy are fully oscillated in the case of vacuum oscillations. Thus Data/SSM of all the existing experiments should be same and the different Data/SSM among the experiments are hardly explained. One of the scenario is that Δm^2 and $\sin^2 2\theta$ eventually take "good" values, for example $(\Delta m^2, \sin^2 2\theta) \sim (10^{-10}, 1)$, to explain all the results. This scenario is so-called the just-so oscillation. Figure 3, taken from Ref.8 shows the 95% C.L. allowed regions of just-so solution in (Δm^2, $\sin^2 2\theta$) space. The other attractive scenario which could explain all the experimental results is matter enhanced oscillations of solar neutrinos, so-called MSW oscillation.[9] Figure 4, taken from Ref.[8] shows the 95% C.L. allowed regions of MSW solution in (Δm^2, $\sin^2 2\theta$) space. There are two domains of allowed regions, so called small angle solution and large angle solution. It is predicted that the energy spectrum of solar neutrinos would be distorted in the case of the small angle solution. On the other hand, the day/night effect, that is, a difference between day and night flux, would

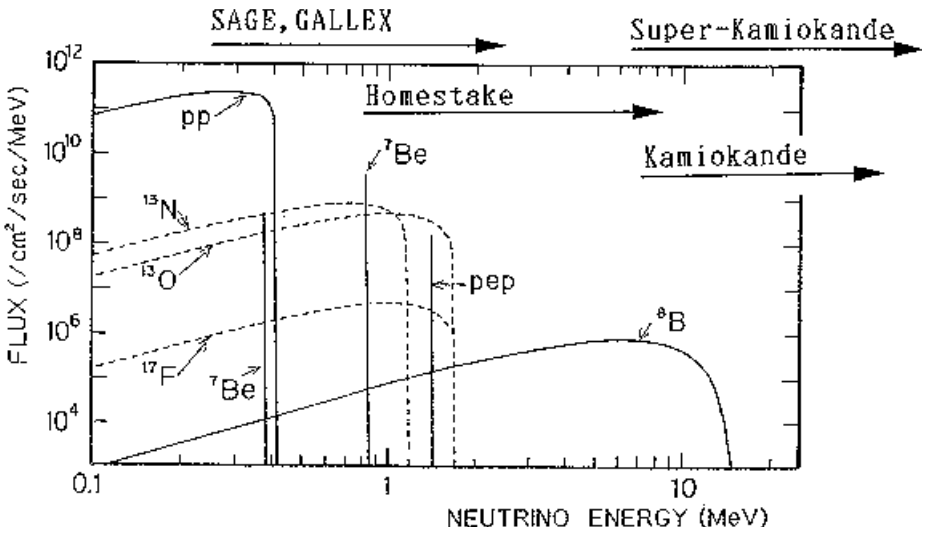

Figure 2: The energy spectra of the solar neutrino flux. Also shown are the energy threshold of the existing solar neutrino experiments.

be observed in the case of the large angle solution. Real-time measurement of solar neutrino is indispensable to detect those effects, which would be a strong evidence of MSW oscillation. Super-Kamiokande can provide a huge statistics for those measurement with its large fiducial mass.

The presented solar neutrino data of 374.2 live-days, covering a period from May 31, 1996 through Oct 20, 1997. First, cosmic ray muons and decay electrons are discarded from the data sample using total energy deposit in the detector and time difference of the events. The vertex position of ν-e scattering and the direction of electrons have been reconstructed by using arrival-time information of Čerenkov photons on the PMT's of inner detector. The energy of electron has been determined from a number of hit PMT's in a 50 ns window. The energy scale, the energy resolution, the angular resolution and the vertex position resolution are calibrated mainly with the electron beam from a LINAC system. The LINAC system can produce an electron beam of 5$\sim$16 MeV injected to various positions in the detector. The energy, angular and position resolutions for 8.6 MeV electrons are 16 %, 27 deg. and 85 cm, respectively. The uncertainty of absolute energy scale is $\pm$1 %. Both of the position dependence and time variance of the energy scale are $\pm$1%, which has been checked with a Ni-Cf source by using the reaction Ni(n,γ)Ni. To eliminate the background

Target(Exp.)	Data	SSM (BP-95)	Data/SSM$^{(*)}$
^{71}Ga(SAGE)	$69\pm10^{+5}_{-7}$	137^{+8}_{-7}	$0.504^{+0.082}_{-0.089}$
^{71}Ga(GALLEX)	$69.7\pm6.7^{+3.9}_{-4.5}$	137^{+8}_{-7}	$0.509^{+0.057}_{-0.059}$
^{37}Cl(Homestake)	$2.55\pm0.14\pm0.14$	$9.3^{+1.2}_{-1.4}$	0.273 ± 0.021
$e^-(H_2O$,Kamiokande)	$2.80\pm0.19\pm0.33$	$6.62^{+0.93}_{-1.12}$	0.423 ± 0.058
$e^-(H_2O$,Super-Kam.)$^{(**)}$	$2.37^{+0.06+0.09}_{-0.05-0.07}$	$6.62^{+0.93}_{-1.12}$	$0.358^{+0.017}_{-0.013}$

(*) Experimental errors only. Statistical and systematic errors are added in quadrature.

(**) Preliminary.

Table 1: Results from current five experiments and the SSM[2] BP-95 predictions on the solar neutrino flux. Here the unit is SNU for ^{37}Cl and ^{71}Ga and $10^6\nu/\mathrm{cm}^2/\mathrm{sec}$ for $e^-(H_2O)$ target, respectively, where SNU means "solar neutrino unit" defined by 1 SNU=10^{-36} ν captures per atom per second.

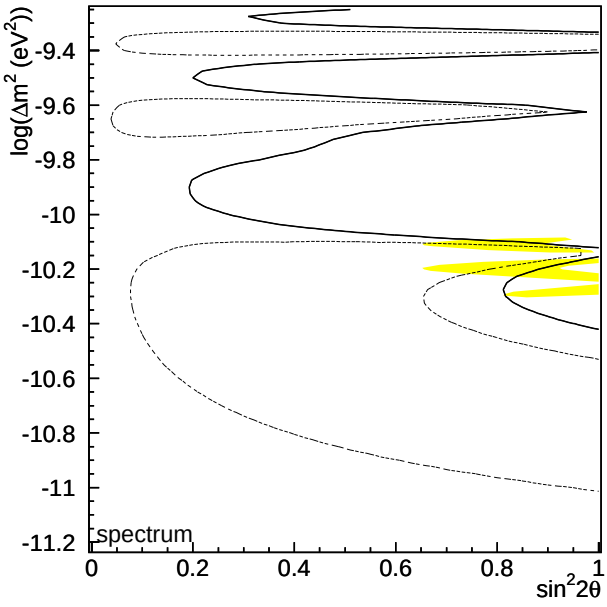

Figure 3: The 95 % C.L. allowed region of just-so oscillation by Hata and Langacker[8] are shown by the shaded region. Also shown are the preliminary 95% C.L. and 99% C.L. contours at just-so region from spectrum analysis without flux constraint in Super-Kamiokande. Insides of dashed lines are allowed at 95% C.L., and right side of solid line is excluded at 99% C.L. from spectrum analysis.

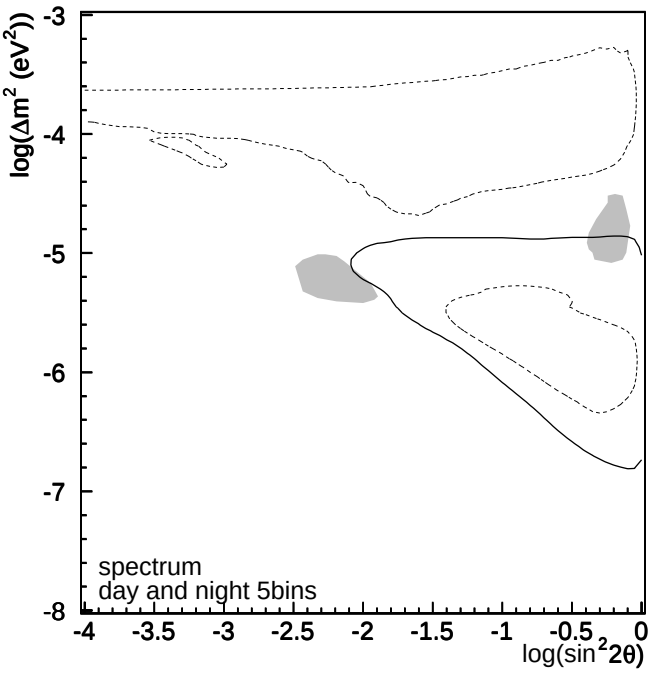

Figure 4: 95% C.L. allowed region of MSW oscillation by Hata and Langacker[8] are shown by the shaded region. Also shown is 95% C.L. excluded region of MSW oscillation analysis without flux constraint in (Δm^2,$\sin^2 2\theta$) space. Day/night analysis excludes region inside of solid line and spectrum analysis excludes regions inside of dashed lines.

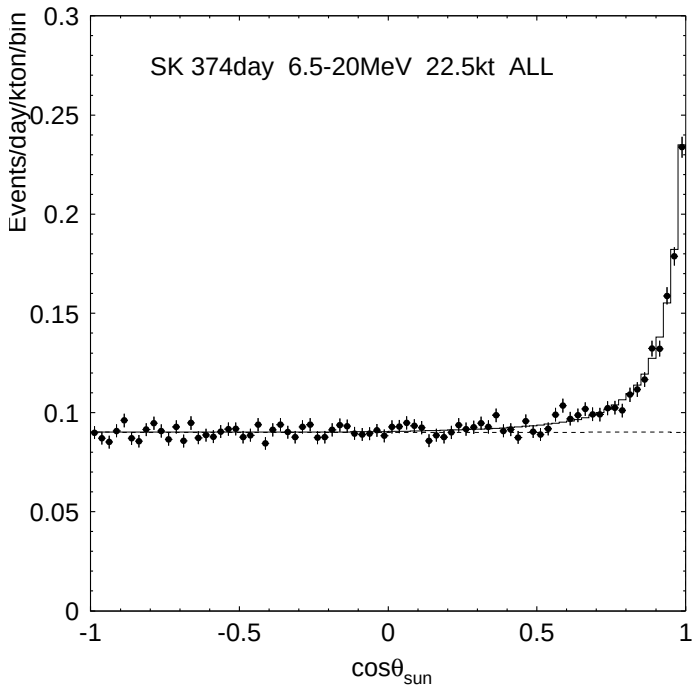

Figure 5: Preliminary solar neutrino data from the Super-Kamiokande experiment in 374.2 days of observation. A clear excess of events near $\cos\theta_{sun}$ =1 is seen. The shape of the excess distribution is reproduced well by the MC simulation with the ^{8}B flux of 0.358×SSM.

events due to activity from surrounding rocks, we required a distance of the vertex from the inner detector wall is more than 2 m. This corresponds 22.5 kt as a fiducial mass. Another background due to the activity from nuclear fragments produced by μ spallation has been reduced by checking the distance and time interval between a event and a prior cosmic ray μ event. Finally the distribution of directional correlation to the Sun has been obtained for the events where energy of electrons are between 6.5 and 20 MeV as shown in Fig. 5. The number of obtained solar neutrino events is $4951.8^{+117.9}_{-111.3}$(stat.)$^{+444}_{-154}$(syst.) which corresponds to $2.37^{+0.06}_{-0.05}$(stat.)$^{+0.09}_{-0.07}$(syst.) $\times 10^6$/cm^2/s as a ^{8}B-neutrino flux. The obtained Data/SSM is $0.358^{+0.009}_{-0.008}$(stat.)$^{+0.014}_{-0.010}$(syst.). The presented result of total flux is consistent to the previous result observed in Kamiokande. Note that the number of obtained solar neutrinos by Super-Kamiokande in 1.5 year operation is more than eight times larger than that by Kamiokande in seven years operation.

The flux difference between day and night is expressed as: (Day-Night) /

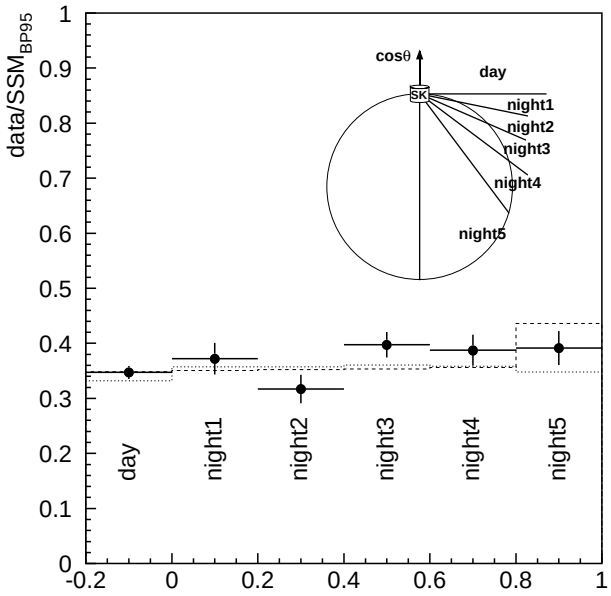

Figure 6: Preliminary reslts in Day/Night effect. Error bars are statistical only. Night data is divided into 5 bins. Night1 is horizontal direction and night5 is vertical direction. The histogram with dotted lines is the expected variation of the typical large angle solution and histogram with dashed lines is that of the typical small angle solution (see text).

(Day+Night) = -0.031±0.024(stat.)±0.014(syst.). Within the statistics, there is, so far, no evidence for the day/night effect. Figure 2 shows the solar neutrino flux in day and night periods. The night and day flux are subdivided into 5 bins according to the angle between the direction to the Sun and the nadir of the detector. The 5-binned histograms expected from MSW oscillation with typical parameters in the small mixing solution, $(\Delta m^2, \sin^2 2\theta) = (9.12 \times 10^{-3}, 6.31 \times 10^{-6})$ and in the large angle solution, $(\Delta m^2, \sin^2 2\theta) = (2.82 \times 10^{-5}, 0.66)$ are also shown in the figure. The data seems to agree with no day/night effect, but also to agree with the day/night effect with some parameters of the large angle solution. The implication in the MSW oscillation has been performed for the 5-binned day/night result as shown in Fig 2. This analysis is a model independent analysis, since only the variation of ^{8}B-neutrino flux between day and night is used. The excluded

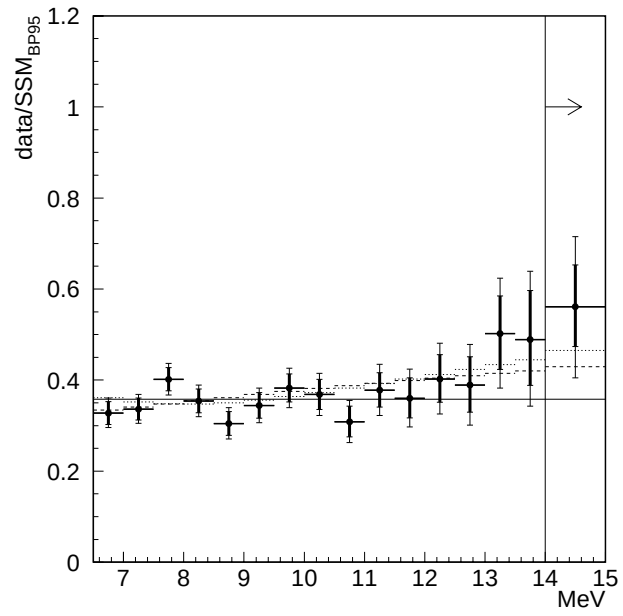

Figure 7: Preliminary plot of Data/SSM as a function of electron energy from Super-Kamiokande. The most right bin shows the data with electron energy more than 14 MeV. Inner error bars are the statistical ones and outer bars are the systematic errors added linearly with statistical ones. Dashed histogram is the expected spectrum of the typical small angle solution and dotted histogram is that of the typical just-so solution (see text).

region at 95% C.L. from the analysis of obtained results in day/night effect are plotted in Figure 4. The presented results have excluded lower Δm^2 region in the large angle solution.

Figure 7 shows Data/SSM as a function of electron energy. The inside error bars show statistical errors, and outside bars show the systematic error mainly due to uncertainty in the energy scale and energy resolution. These systematic errors are fully correlated to the energy of electrons. Also shown are the expected spectrum of typical small angle solution, $(\Delta m^2, \sin^2 2\theta)=(9.12\times10^{-3},\ 6.31\times10^{-6})$ and the typical just so oscillation, $(\Delta m^2, \sin^2 2\theta)=(7.08\times10^{-11},\ 0.83)$. There appears to be no significant distortion in the obtained spectrum. However, it is interesting that possible distorted spectra by neutrino oscillations, for example as shown in the figure, also agree with data and even give better χ^2 for the fitting. The model independent implication of the energy spectrum has been performed

in MSW parameter region and in just-so parameter region. We have not used the constraint to ^{8}B-neutrino flux from SSM due to 20 % uncertainty for the analysis. The contour plots for MSW oscillation and for just-so oscillation are shown in Fig. 4 and in Fig. 3, respectively. The absence of significant distortion of the energy spectrum excludes some region in both of the parameter space. Because of a good fit of the spectrum in just-so region, the 95 % C.L. allowed region appears as shown in Fig 3, though the no oscillation hypothesis is still allowed at 99 % C.L.

3 Atmospheric neutrino

Atmospheric neutrinos are produced by the decay of π or K produced by the interaction of primary component of cosmic ray in the atmosphere. The typical altitude where atmospheric neutrinos are produced is 10 km so that the typical flight length of neutrinos is $\sim$ 10 km for downgoing ones and $\sim 10^4$km for upgoing ones. The ν_μ/ν_e ratio of the atmospheric neutrino flux below a few GeV is roughly 2, since π decay is dominant and the $\pi \to \mu \to e$ decay chain as following is $\pi^\pm \to \mu^\pm + \nu_\mu(\bar{\nu_\mu}), \mu^\pm \to e^\pm + \nu_e(\bar{\nu_e}) + \bar{\nu_\mu}(\nu_\mu)$. (Hereafter ν represents $\nu + \bar{\nu}$.) It goes up more than 2 for higher energy neutrinos since high energy μ's hits grounds before their decay. The total flux of atmospheric neutrinos has been calculated by several model. The uncertainty of the flux is about 20%, while the uncertainty of ν_μ/ν_e ratio is 5 % below a few GeV region. To cope with detection efficiency of the detector, the "double ratio R" defined as;

$$R = \frac{(\nu_\mu/\nu_e)_{data}}{(\nu_\mu/\nu_e)_{MC}}, \tag{1}$$

is often used. If $(\nu_\mu/\nu_e)_{data}$ is consistent with the prediction, R should take unity.

In recent years, there have been several measurements of ν_μ/ν_e ratio by water Čerenkov detectors, IMB-3[10],[11] Kamiokande,[12] and tracking type detectors, NUSEX,[13] Frejus[14] and Soudan-2.[15] Two water Čerenkov experiments, Kamiokande and IMB, have obtained consistent result which is substantially smaller than unity. The anomaly of μ/e ratio can be interpreted as possible neutrino oscillation, for example, $\nu_\mu \to \nu_e$ or $\nu_\mu \to \nu_\tau$. On the other hand, the result of NUSEX and Frejus seems to be consistent with unity, while their statistics are not sufficient for conclusive result. Furthermore, recent data from Soudan-2 agree with the data from the water Čerenkov detectors, although the value of unity is still allowed at

Table 2: Experimental results on the atmospheric (ν_μ/ν_e) ratio.

Exp.	Data		MC		$(\mu/\mathrm{e})_{data}/(\mu/\mathrm{e})_{MC}$	
	e-like	μ-like	e-like	μ-like		
NUSEX	18	32	20.5	36.8	$0.99^{+0.35}_{-0.25}\pm$?	
Frejus	75	125	81.4	136.2	$1.00\pm0.15\pm0.08$	
Soudan-2	79.1	54.6			$0.67\pm0.15^{+0.04}_{-0.06}$	
IMB-3(sub-GeV)	325	182	257.3	268.0	$0.54\pm0.05\pm0.12$	
(multi-GeV)	25	47	30.8	41.2	$1.40\pm0.66\pm0.21$	(*)
Kamiokande(sub-GeV)	248	234	227.6	356.8	$0.60^{+0.06}_{-0.05}\pm0.05$	
(multi-GeV)	98	135	66.5	162.2	$0.57^{+0.08}_{-0.07}\pm0.07$	
Super-Kam.(sub-GeV)(*)	983	900	812.2	1218.3	$0.61^{+0.029}_{-0.028}\pm0.049$	
(multi-GeV)(*)	218	176	182.7	229.0	$0.64^{+0.069}_{-0.062}\pm0.097$	
(PC)(*)	—	200	—	244.8	$0.67^{+0.059}_{-0.054}\pm0.081$(**)	

Preliminary.

(**) The double ratio is for the combined sample of FC and PC events.

2σ level. Though the theoretical uncertainty of absolute flux and interaction cross sections of neutrinos are large, they should cancel in the double ratio. Hence, the small double ratio can be considered as possible evidence of $\nu_\mu \to \nu_e$ or $\nu_\mu \to \nu_\tau$ oscillations.

Another indication of the oscillation of atmospheric neutrinos is the distortion of zenith angle distribution of neutrino flux. The flux of atmospheric neutrinos depends on zenith angle. This dependence is caused by the difference of effective thickness of atmosphere. Hence, the shape of zenith angle distribution should be symmetric for upgoing versus downgoing neutrinos. Typical E/L for atmospheric neutrinos, for example, of 1 GeV is 10^{-1} for downgoing and 10^{-4} for upgoing. Therefore, possible distortion of zenith angle distribution is clear evidence of neutrino oscillations. Only the Kamiokande experiment has reported the zenith angle distributions of neutrino flux for the time being.[12] They reported a possible distortion of zenith angle distributions in multi-GeV sample (E_ν higher than roughly 1 GeV), which suggests the neutrino oscillation with $\Delta m^2 \sim 10^{-2}$ eV^2 and with the large mixing angle as shown in Fig. 8. Much more data are needed to establish the oscillation of atmospheric neutrinos. Super-Kamiokande can collect large statistics which are indispensable to test the oscillation hypothesis and to derive

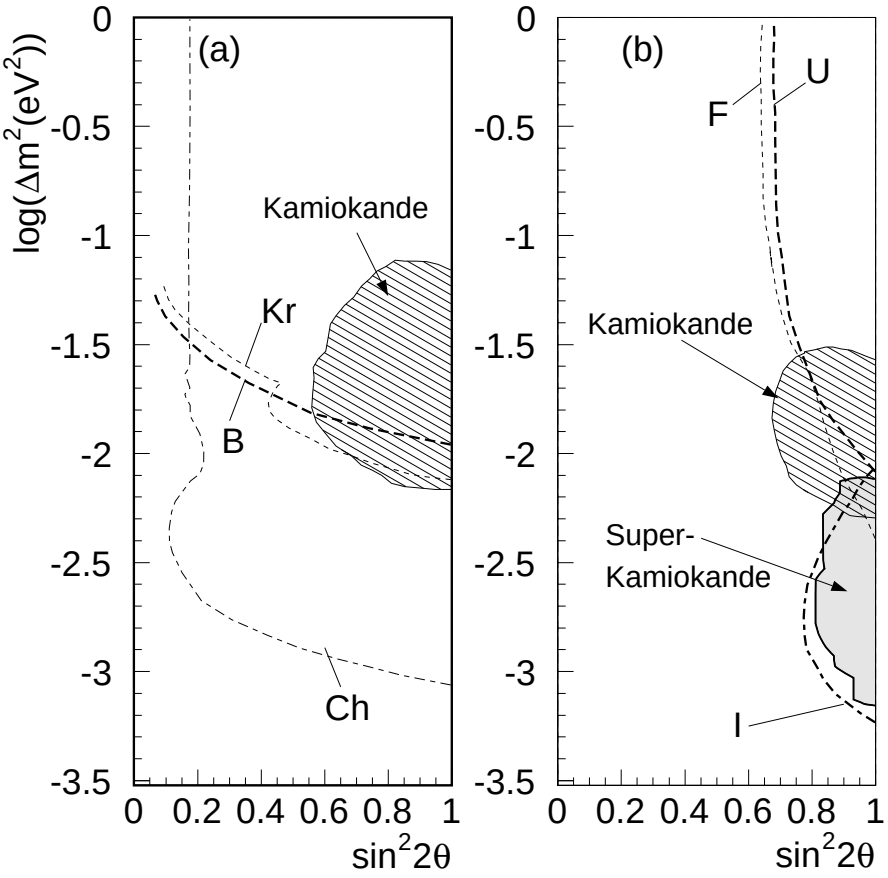

Figure 8: Allowed regions (90 % CL) in the (Δm^2, $\sin^2 2\theta$) space (a) for $\nu_\mu - \nu_e$ oscillation and (b) for $\nu_\mu - \nu_\tau$ oscillation. Regions with diagonal lines show the allowed regions obtained by Kamiokande[12]. The shaded region in (b) is the preliminary allowed region by Super-Kamiokande. Other lines indicate the regions above and to their right are excluded; B, Bugey reactor experiment[16]; Kr, Krasnoyarsk reactor experiment[17]; Ch, Chooz reactor experiment[18]; F, Frejus fully-contained atmospheric neutrinos[14]; U, compilation of upward through-going muons data[19]; I, IMB upward stopping muons[20]. Super-Kamiokande's analysis on $\nu_\mu - \nu_e$ oscillation was not ready.

the oscillation parameters from double ratio and zenith angle distribution.

We have analyzed fully-contained (FC) events of 414.2 live days (25.5 kton-years) and a partially-contained (PC) events 370.8 live days (22.8 kton-years). In a FC event, all the charged particles are contained in the inner detector and the total energy of the event is fully reconstructed. In a PC event, one charged particle, usually μ, escapes from the inner detector and deposits energy in the outer detector. To separate a FC event from a PC event, we have required total number of hits in a spatial cluster in the outer detector to be less than 10. Both FC and PC events have been doubly scanned by physicists to eliminate background events due to detector noise. Then the vertex position of the neutrino interaction and Čerenkov rings have been reconstructed automatically by a computer. The vertex position resolution is estimated to be 30 cm for single ring FC events. The angular resolution of single ring FC events is estimated to be 3 degrees. Finally, a 2 m fiducial cut has been applied for events in both the FC and PC samples. Total visible energy cuts, $E_{vis} \geq 30$ MeV and $E_{vis} \geq 350$ MeV have been applied for the FC and the PC sample, respectively. The accuracy of the absolute energy scale is estimated to be ± 2.4 % based on several calibration sources: cosmic ray through-going muons, stopping muons, muon-decay electrons, the invariant mass of π^0's produced by neutrino interactions, Ni-Cf source calibration, and the 5-16 MeV LINAC. The momentum of particles are determined from the total number of photo-electrons within a 70 degrees half-angle cone relative to the track direction. The estimated momentum resolution for electrons and muons is $2.5\%/\sqrt{E}+0.5$ % and 3 %, respectively, where E is the energy of electron in GeV unit. After those reductions, the number of neutrinos is 3,462 for the FC sample and 200 for the PC sample. Events per day is 8.4 for the FC sample and 0.54 for the PC sample.

In the FC events, single ring events have been selected. Figure 9 shows a typical single ring "μ-like" event and an "e-like" event. There is a difference between the shape of rings in the figure, since a Čerenkov ring from electromagnetic cascades cause a more diffuse photon distribution than that from muons. The particle identification (PID) method which uses the distribution of Čerenkov photons in a ring as well as the opening angle of the ring are applied to distinguish muons from electrons. Figure 10 shows the result of PID for single ring FC events. Those two peaks corresponding to μ and e are clearly separated in these distributions. The probability of mis-identification deduced from MonteCarlo is less than 0.5% for the single ring FC sample. The PC events are regarded as μ-like events, since

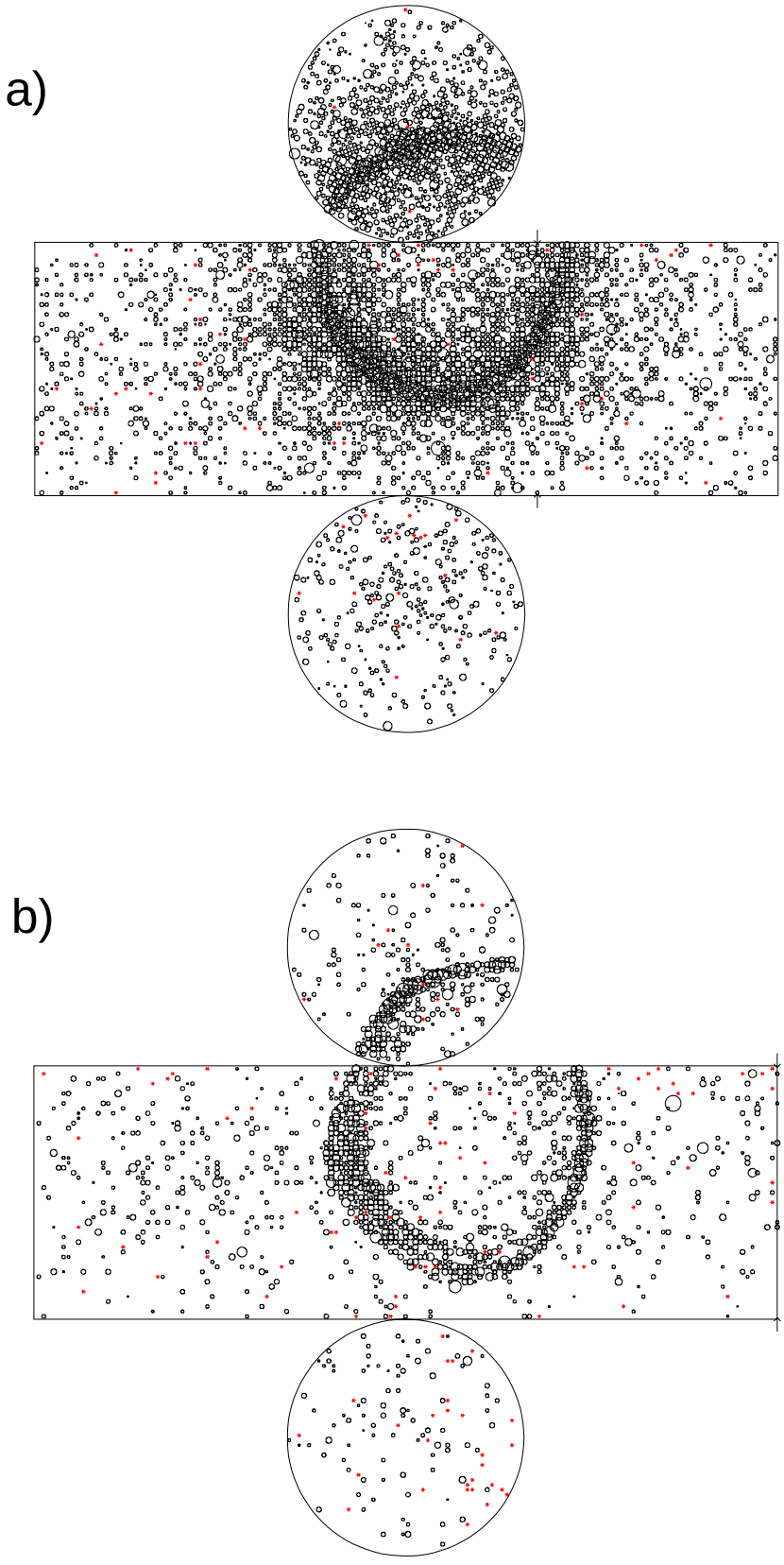

Figure 9: Typical samples of a) 1 ring e-like event and b) μ-like event

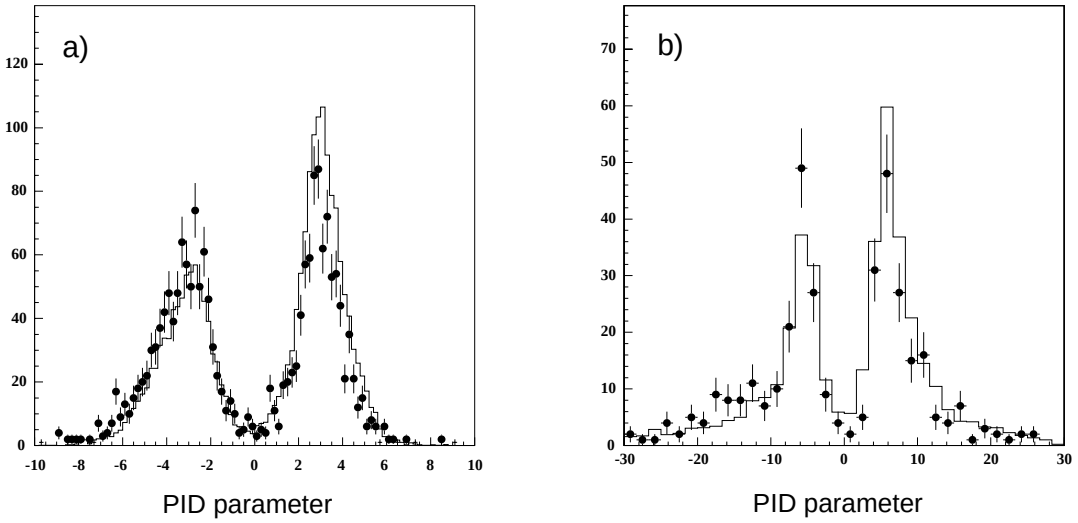

Figure 10: Distribution of the PID parameter for μ-like events (PID<0) and for e-like events (PID>0) in a) sub-GeV sample and in b) multi-GeV sample. The closed circles and histograms are for the data and for Monte Carlo events, respectively.

97% of the PC events are caused by charged current ν_μ interactions.

Table 2 shows the final results of two different energy regions, namely sub-GeV and multi-GeV, according to the definition of selection criteria used in Kamiokande. The sub-GeV sample is the subset of FC events where 1) E_{vis} < 1.33 GeV, 2) P_e > 100 MeV/c for e-like events, and 3) P_μ > 200 MeV/c for μ-like events. In sub-GeV sample, the numbers of single ring e-like and μ-like events are 983 and 900, respectively, while the expected numbers using Honda's flux are 812.2 and 1218.3 for the single ring e-like and μ-like events, respectively. The multi-GeV sample is the subset of FC events with $E_{vis} \geq 1.33$ GeV. The number of single ring e-like and μ-like events are 218 and 176, respectively, while the expected numbers are 182.7 and 229.0. The number PC events is 200, while the expected number is 244.8. Those numbers are summarized in Tab. 2. As shown above, Super-Kamiokande observed small double ratios for both the sub-GeV and the multi-GeV energy sample. The double ratio are $0.611^{+0.029}_{-0.028}\pm0.049$ and $0.665^{+0.059}_{-0.054}\pm0.081$ for the sub-GeV FC sample and combined sample of multi-GeV FC and PC, respectively. Obtained double ratios in Super-Kamiokande are therefore inconsistent with unity, and consistent with the previous results of wa-

ter Čerenkov experiments. Thus, the atmospheric neutrino anomaly has been established.

Fig. 11 shows the momentum distribution for the FC events. One can see that the shape of the distributions for the e-like and μ-like events are reproduced well by the Monte Carlo. We can not determine whether ν_μ deficit or ν_e excess takes place due to 25 % uncertainty in absolute normalization coming from uncertainty of neutrino flux and of neutrino interaction cross sections. The deficit(excess) of events in the muons (electrons) of the data, however, can not be explained within a 5 % uncertainty of expected μ/e ratio. Figure 12 shows the double ratio vs lepton momentum in both of the samples. It appears that the small double ratio does not depend strongly on the momentum. Figure 13 shows the double ratio vs D_{wall}, distance from the inner wall. Each bin of D_{wall} is chosen to give the same fiducial mass. It is clear that the double ratio is not dependent on the vertex position. This proves the obtained small double ratios are not due to contamination from any kind of incoming particles like cosmic ray muons or neutrons from rock.

The higher energy neutrinos have the better angular correlation to the lepton produced via CC interaction. For example, the angle between the neutrino and the lepton is roughly 20 degrees in multi-GeV sample. The direction of neutrinos can be measured by using the direction of a single ring. Fig. 14 shows the zenith angle distribution of μ-like events and e-like events in sub-GeV and multi-GeV + PC samples together with Monte Carlo expectations. A large deficit of upward going neutrinos are significantly observed in the multi-GeV μ-like sample. Note that any systematic effects due to the cross section and neutrino flux calculation are canceled in the symmetry of the zenith angle distribution, and cannot explain the presented large distortion. The hypothesis of neutrino oscillations can naturally explain this asymmetry. Preliminary oscillation analysis assuming $\nu_\mu \rightarrow \nu_\tau$ oscillation has been made. The 90 % C.L. allowed region is shown in Fig 8. Although the suggested region is slightly lower in Δm^2 than that of Kamiokande, the overlap region with the Kamiokande result appears at around 5×10^{-3} eV^2.

4 Results in upward-going muons

Another indication of neutrino oscillations can be derived from upward-going muon data. The upward-going muons are produced by charged current ν_μ interactions in the rock near the detector. If the energy of muons is larger than several

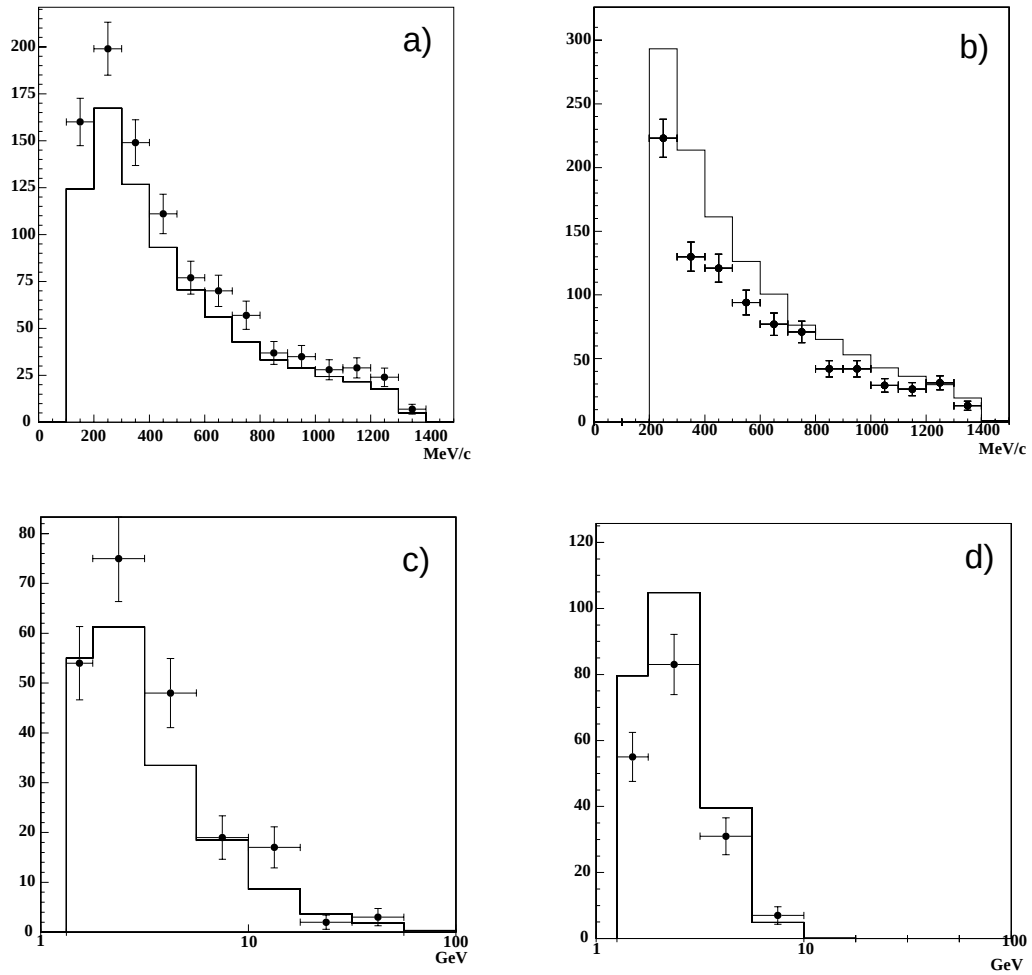

Figure 11: Momentum distribution for (a)e-like and (b)μ-like events in the sub-GeV sample and c) e-like and d) μ-like events in the Multi-GeV sample from Super-Kamiokande. The histograms show the MC prediction.

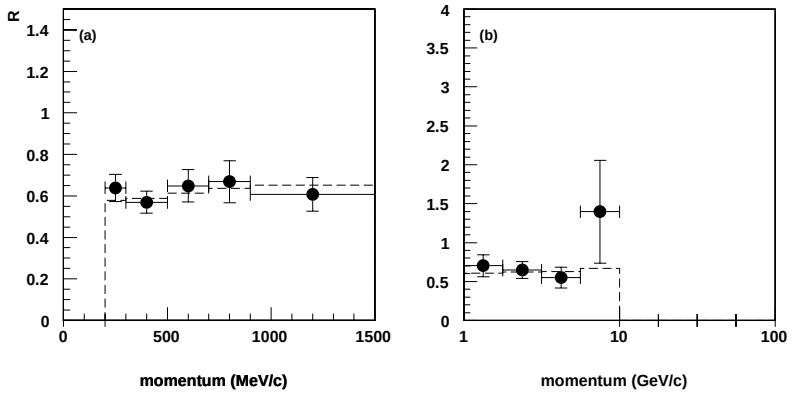

Figure 12: The momentum dependence of the double ratio R for a) sub-GeV and b) multi-GeV. The closed circles show the data. The histograms with dotted line show the expected one with $\nu_\mu \rightarrow \nu_\tau$ oscillation in the case of $(\Delta m^2, \sin^2 2\theta) = (5 \times 10^{-3}, 1.)$.

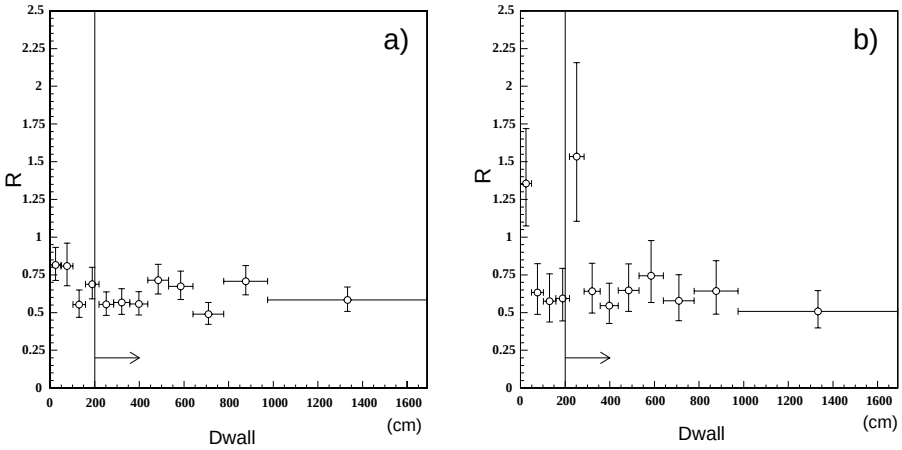

Figure 13: The double ratio R in each D_{wall} bin for a) the sub-GeV and b) the multi-GeV sample. The 2m fiducial volume cuts are also shown.

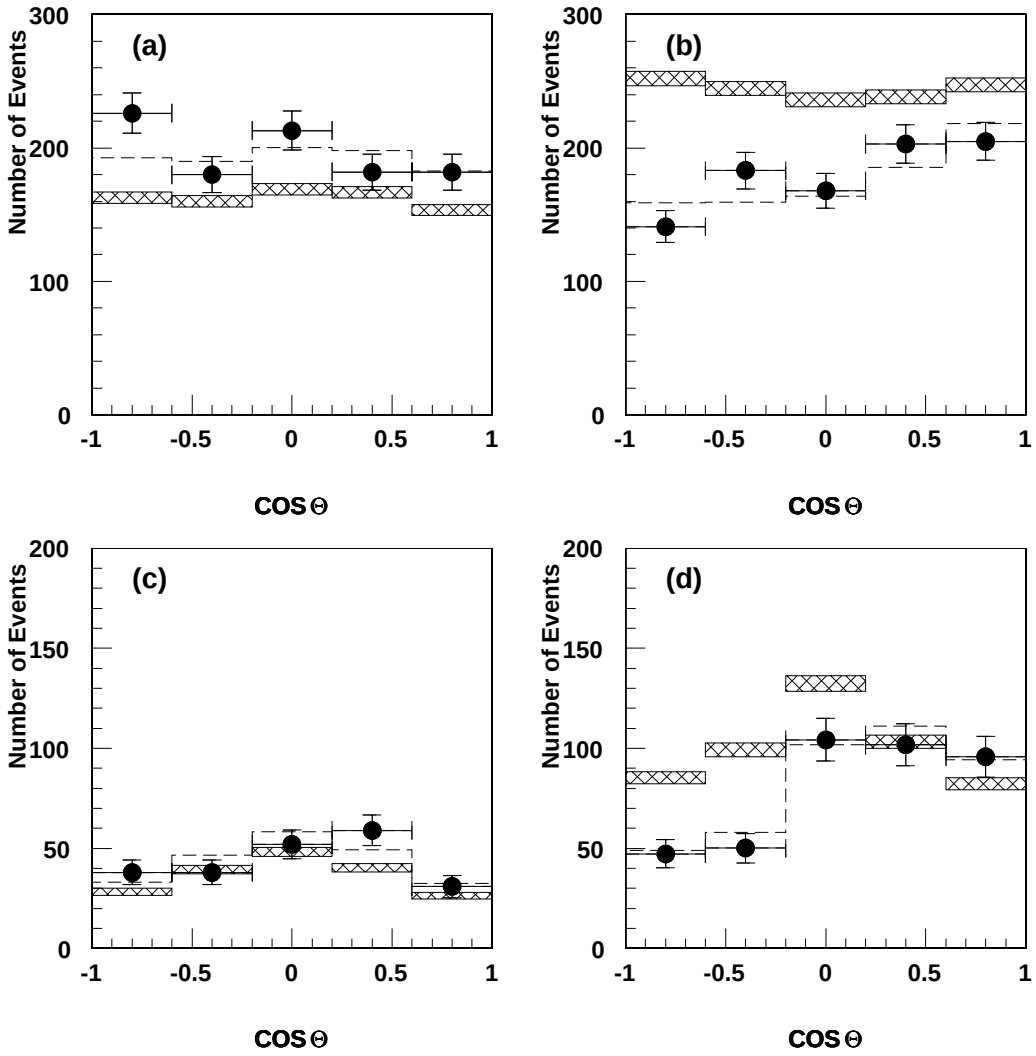

Figure 14: The double ratio R as a function of zenith angle for (a)sub-GeV e-like, (b) sub-GeV μ-like, (c) multi-GeV e-like, (d) multi-GeV μ-like events. Histograms with solid line show the expectation from Monte Carlo without oscillations. The hatched boxes show the errors due to Monte Carlo statistics. Histogram with dashed line show the expectation with $\nu_\mu \to \nu_e$ oscillation with $(\Delta m^2, \sin^2 2\theta) = (5 \times 10^{-3}, 1.)$. Cos$\Theta$ =1 corresponds to down going particles.

GeV, they pass through the detector. These are called upward-going-through muons. The typical neutrino energy is the order of 100 GeV for upward-going-through muons.

Upward-going through muons have been selected in 362 live days data sample. All the direction and entering position of muons have been reconstructed automatically by a program, then later by manual fitting to measure them more precisely. Cosmic ray muons, which are the main background events, have been easily rejected by applying the zenith angle cut ($\cos\theta_z \leq 0$). The path length of the muon track in the inner detector has been required to be more than 7 m. This corresponds to a 1.7 GeV cut. The total observed number of upward-going-through muons is 409 in 362 live days. The expected number of upward-going through muons from a calculation is 445 ± 89. It is hard to compare the obtained number of upgoing muons to the expected one since absolute number has about 20 % uncertainty due to the flux of atmospheric neutrinos and the cross section. However, possible distortion of zenith angle distribution is free from such systematics, and could be evidence of neutrino oscillations just as in the vertex-contained event data.

Figure 15 shows the zenith angle distribution obtained from Kamiokande and from Super-Kamiokande together with the expectation. The closed circles and open circles show the data of Kamiokande and of Super-Kamiokande, respectively. Those data of two experiments agree well. The expected distributions in the case of no oscillation and the oscillation with $(\Delta m^2, \sin^2 2\theta) = (5 \times 10^{-3}, 1.)$. for both experiments are also shown with thin solid lines and with thin dashed lines, respectively. Those plotted histograms are best-fitted ones within 20 % uncertainty in absolute normalization. The data of two experiments are consistent with each expectation with no oscillation with in errors, though the statistics is not enough so far. However, it is interesting that the hypothesis of $\nu_\mu \rightarrow \nu_x$ oscillation with the parameter suggested by the contained data, for example (Δm^2, $\sin^2 2\theta$)=$(5 \times 10^{-3}$ eV^2,1.), agrees well with the data, or, even fits better. Apparently much more statistics and further study of systematic error are needed to give a decisive answer for neutrino oscillations.

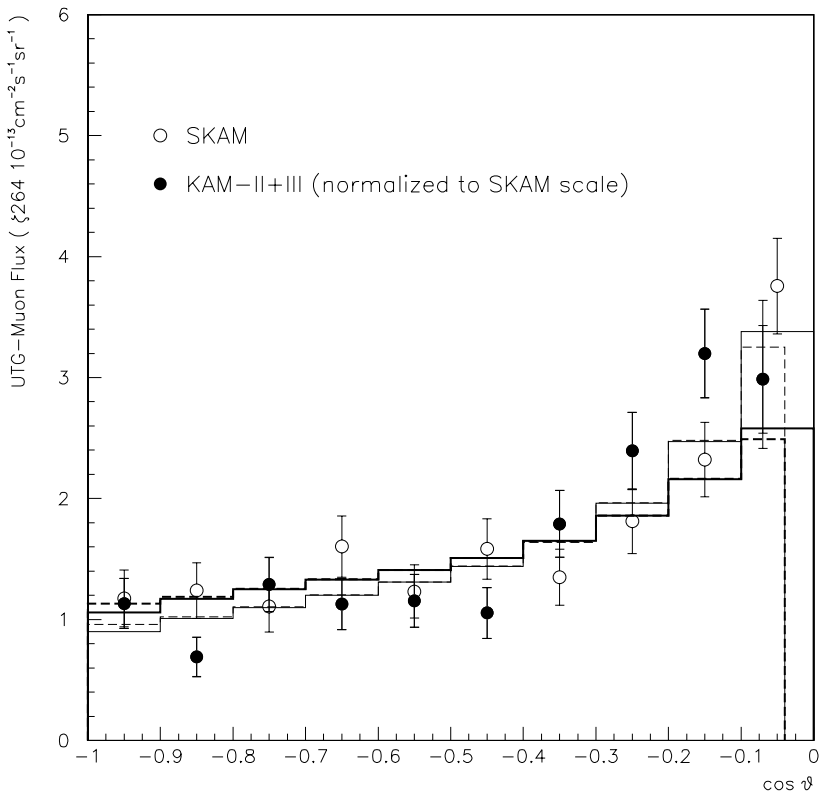

Figure 15: The zenith angle distribution of upward going through muons from Kamiokande (full circle) and Super-Kamiokande (open circle). Histograms show the expected distributions from no oscillation (thick solid and dashed lines for Super-Kamiokande and Kamiokande, respectively) and from $\nu_\mu - \nu_\tau$ oscillation with $\Delta m^2 = 5 \times 10^{-3}\,\mathrm{eV}^2$ and $\sin^2 2\theta = 1$ (thin solid and dashed lines for Super-Kamiokande and Kamiokande, respectively). The results and expected lines for Kamiokande were multiplied by a factor 0.819 to scale its geometrical effect to Super-Kamiokande. The expected lines are the best fitted ones obtained within the absolute scale uncertainty of 20%.

4.1 Future long-baseline experiment at KEK

The effect of neutrino oscillation suggested by the atmospheric neutrino data can be studied by long-baseline neutrino oscillation experiments using high intensity ν_μ beam. One of the possible experiment is the one between KEK-PS and Super-Kamiokande (called K2K).[21] It has the baseline length of 250 km and the average energy of ν_μ beam is roughly 1.5 GeV so that it is just sensitive to the $\Delta m^2 \sim 10^{-2}$ eV^2 region suggested by the Super-Kamiokande data.

The 12 GeV proton beam is extracted from KEK-PS within 1 μsec by every 2 seconds. π^+'s produced by 12 GeV protons are focused by horn magnets and decay into $\mu^+\nu_\mu$ in the 200 m long decay tunnel. The fraction of ν_e in the beam is less than 1 %. There are two kind of beam monitors, the π monitor and the μ monitor, in the decay tunnel. The π monitor downstream the horn magnets is a gas Čerenkov detector which measures the emission angle of Čerenkov photons produced by the π beam with various gas pressure. This monitor provides the information about distribution of momentum and divergence of π beam. The μ monitor downstream the beam dump measures the profile of μ's from the π decays. Those two monitors are useful to understand production of ν_μ beam.

There is a front detector 300 m apart from the target to measure initial flux of ν_μ beam. The front detector consists of the Fine Grain Detector and 1000 ton water Čerenkov detector. The Fine Grain Detector is a tracking-type detector which consists of a "sandwich" of scintillating fiber tracker and water layer as a target. The aim of the detector is to measure the absolute ν_μ flux with 5 % accuracy by choosing quasi-elastic CC interaction. The 1000 ton water Čerenkov detector has the same configuration as Super-Kamiokande. The aim of the detector is to study the detector response which is characteristic for water Čerenkov technique with neutrino beam well-measured by the Fine Grain Detector.

The number of charged current interactions at Super-Kamiokande is about 350 for 10^{20} protons on target (POT) in two years of running. This experiment can search for $\nu_\mu \rightarrow \nu_e$ and $\nu_\mu \rightarrow \nu_\tau$ independently. $\nu_\mu \rightarrow \nu_e$ oscillation can be observed as an appearance of e-like events at Super-Kamiokande. $\nu_\mu \rightarrow \nu_\tau$ oscillation can be observed as possible distortion of ν_μ energy spectrum which can be reconstructed from single ring μ-like events at Super-Kamiokande. Figure 16 shows reconstructed energy spectrum of ν_μ's with no-oscillation and with oscillation. One can see the significant distortion in the spectrum in the case of

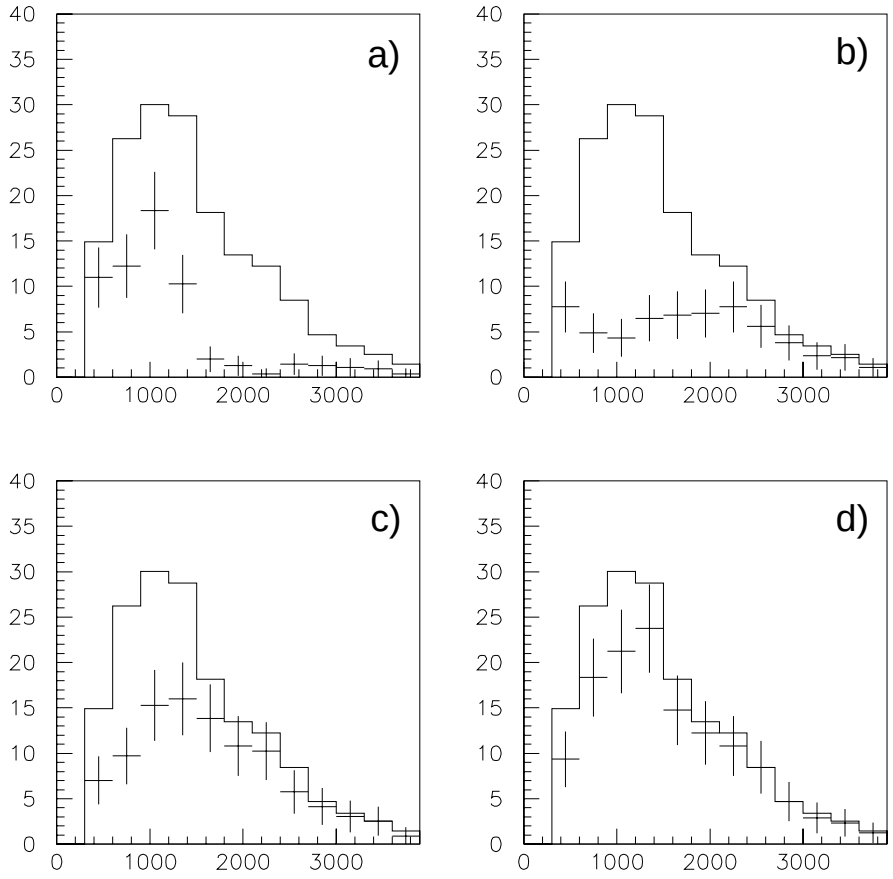

Figure 16: The expected energy distribution of ν_μ at Super-Kamiokande reconstructed from single ring μ-like events. The histograms show the data without oscillation. The crosses shows the data in the case of $\nu_\mu - \nu_\tau$ oscillation with $\sin^2 2\theta = 1$ and a) with $\Delta m^2 = 10^{-2}$ eV^2, b) with $\Delta m^2 = 5 \times 10^{-3}$ eV^2, c) with $\Delta m^2 = 3 \times 10^{-3}$ eV^2, d) with $\Delta m^2 = 2 \times 10^{-3}$ eV^2.

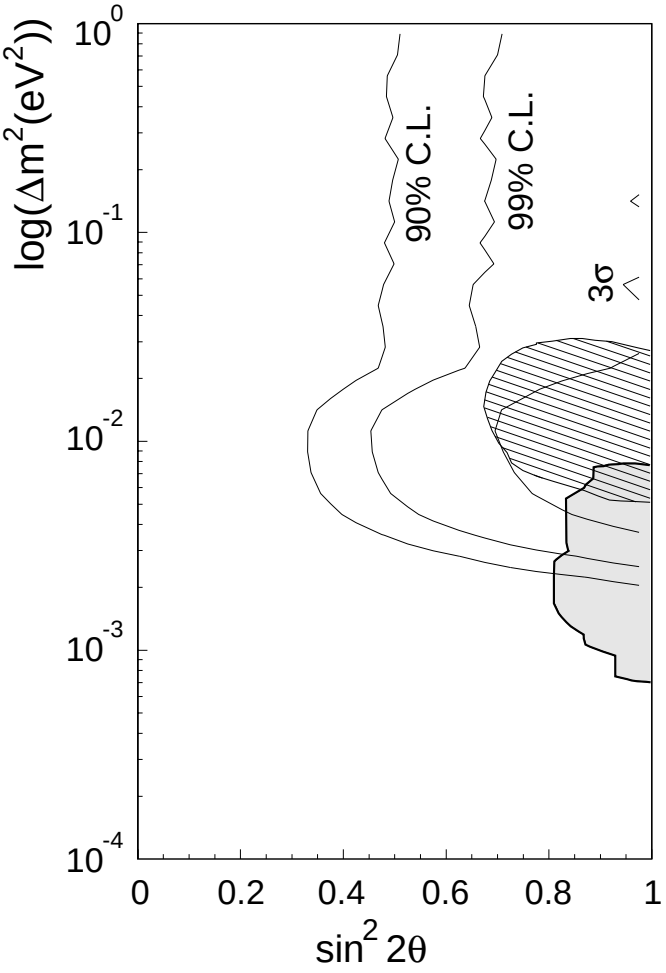

Figure 17: The sensitivity plot in (Δm^2,$\sin^2 2\theta$) space for ν_μ disappearance search with 10^{20} POT by using the neutrino energy spectrum analysis. Each contour at 90 % C.L.,99 % C.L. and 3 σ level is shown. Also shown are the allowed region from Kamiokande and Super-Kamiokande results.

oscillation with Δm^2 suggested by atmospheric neutrino data. The sensitivity for the ν_μ disappearance measurement is plotted in Figure 17. The region where Δm^2 is greater than 3×10^{-3} eV^2 and $\sin^2 2\theta$ is greater than 0.6 can be explored by this experiment.

The construction of the new neutrino beamline has been started in 1996. The installation of the front detector will be started from OCT, 1998. The first neutrino beam will be extracted from Jan,1999. The physics run will be started Apr, 1999 and continues for 2$\sim$3 years. It will give a conclusive result for the oscillation parameter and modes.

5 Conclusion

Super-Kamiokande is the largest underground water Čerenkov detector dedicated to the detection of neutrinos and proton decays. Super-Kamiokande has been continuously running from April 1, 1996 and collects much greater statistics of neutrino data than has been achieved so far by any underground neutrino experiment.

The preliminary results in solar neutrino are reported based on 374 live-days data. The observed flux of solar neutrinos is apparently smaller than the expectation of SSM, and consistent to the previous result of Kamiokande. The Day/Night difference is consistent to zero within error. This result partially excludes the lower Δm^2 region in the large-angle solution of MSW. The observed energy spectrum of data/SSM is not significantly distorted with current errors though a fit with a distorted spectrum gives better χ^2 than comparison to the undistorted shape.

The preliminary results in atmospheric neutrinos are presented based on 414 live-days data. The double ratios are measured both in the sub-GeV sample and the multi-GeV sample. Both are apparently smaller than unity and consistent with the previous Kamiokande result. Moreover, a large deficit of upgoing ν_μ is observed in multi-GeV sample. Those anomalies are hard to explain by standard physics and could be evidence of neutrino oscillations. The preliminary results in upward-going-through muons based on 362 days data are also reported. The observed zenith angle distribution is still consistent with the expectation within errors. However, it is also consistent with $\nu_\mu \rightarrow \nu_x$ oscillation with the parameters suggested by the atmospheric result. Much more statistics are needed to give a decisive answer for neutrino oscillations.

The parameter region suggested by atmospheric neutrino result will be explored by the long baseline experiment using a high intensity ν_μ beam from KEK-PS starting in 1999. We may confirm $\nu_\mu \rightarrow \nu_x$ oscillations by detecting a possible distortion of the ν_μ energy spectrum at Super-Kamiokande. It is exciting that oscillations with the parameters (Δm^2,$\sin^2 2\theta$)$\sim$ (5×10^{-3},1), which are allowed by both the Kamiokande and the Super-Kamiokande atmospheric neutrino results, cause large distortion of the ν_μ energy spectrum. Hopefully, we may determine the mode and parameter of neutrino oscillations and open a new field of neutrino physics.

References

[1] The Super-Kamiokande collaboration, Institute for Cosmic Ray Research (ICRR), University of Tokyo, Gifu University, National Laboratory for High Energy Physics (KEK), Kobe University, Miyagi University of Education, Niigata University, Osaka University, Tokai University, Tokyo Institute of Technology, Tohoku University, Boston University, Brookhaven National Laboratory, University of California, Irvine, California State University, Dominguez Hills, George Mason University, University of Hawaii, Los Alamos National Laboratory, Louisiana State University, University of Maryland, State University of New York at Stony Brook, University of Warsaw, University of Washington.

[2] See, for example, J.N.Bahcall and M.H.Pinsonneault, Rev. Mod. Phys. **67** (1995) 781.

[3] K.Lande, to be published in *Neutrino* 96, Proceedings of the 17th International Conference on Neutrino Physics and Astrophysics, Helsinki, Finland, June 1996. See also B.T.Cleveland et al., Nucl. Phys. B (Proc. Suppl.) **38** (1995) 47.

[4] Y.Fukuda et al., Phys. Rev. Lett. **77** (1996) 1683.

[5] J.N.Abdurashitov et al., Phys. Rev. Lett. **77** (1996) 4708.

[6] W.Hampel et al., Phys. Lett. B **388** (1996) 384.

[7] The Super-Kamiokande collaboration, draft in preparation.

[8] See, for example, N.Hata and P.Langacker, Preprint LASSNS-AST 97/29 (May1997), and references therein.

[9] S.P.Mikheyev and A.Yu.Smirnov, Sov. J. Nucl. Phys. **42** (1985) 913; L.Wolfenstein, Phys. Rev. D **17** (1978) 2369; ibid. **20** (1979) 2634.

[10] Becker-Szendy et al., Phys. Rev. D **46** (1992) 3720.

[11] R.Clark et al., to be published in Phys Rev. Lett. R.Clark, private communication for the $(\mu/\mathrm{e})_{data}/(\mu/\mathrm{e})_{MC}$ value.

[12] Y.Fukuda et al., Phys. Lett. B **335** (1994) 237.

[13] M.Aglietta et al., Europhys. Lett. **8**, (1989) 611.

[14] K.Daum et al., Z. Phys. C **66** (1995) 417.

[15] W.W.M.Allison et al., Phys. Lett. B **391** (1997) 491. M.C.Goodmann, for the Soudan-2 collaboration, talk presented at Sixth Conference on the Intersections of Particle and Nuclear Physics, Montana, USA, May-June, 1997.

[16] B. Achkar etal., Nucl. Phys. B **434** (1995)503.

[17] G. S. Vidyakin etal., *Sov. Phys. JETP* **71**, 424 (1990); *JETP Lett.* **59**, 390 (1994).

[18] Chooz collaboration, preprint hep-ex/97110002 (5 Nov 1997)

[19] W. Frati etal., Phys. Rev. D **48** (1993) 1140.

[20] R. Becker-Szendy etal., Phys. Rev. Lett. **69** (1992) 1010.

[21] K.Nishikawa INS-Rep.-924, (1992).